International Conference on Mathematics, Computational Methods & Reactor Physics (M&C 2009)
Saratoga Springs, New York, May 3-7, 2009, on CD-ROM, American Nuclear Society, LaGrange Park, IL (2009)

ADAPTIVE ALGORITHMS FOR A SELF-SHIELDING WAVELET-BASED GALERKIN METHOD

D. Fournier and R. Le Tellier
CEA Cadarache
DEN/DER/SPRC/LEPh
Building 230, 13108 Saint Paul-lez-Durance, France
damien.fournier@cea.fr; romain.le-tellier@cea.fr

ABSTRACT

The treatment of the energy variable in deterministic neutron transport methods is based on a multigroup discretization, considering the flux and cross-sections to be constant within a group. In this case, a self-shielding calculation is mandatory to correct sections of resonant isotopes. In this paper, a different approach based on a finite element discretization on a wavelet basis is used. We propose adaptive algorithms constructed from error estimates. Such an approach is applied to within-group scattering source iterations. A first implementation is presented in the special case of the fine structure equation for an infinite homogeneous medium. Extension to spatially-dependent cases is discussed.

Key Words: Self-shielding, Wavelets, Discontinuous Galerkin Method, Adaptiveness

1. INTRODUCTION

Multigroup discretization is at the basis of the treatment of the energy variable in deterministic neutron transport methods. It consists in considering as constant cross-sections and flux within a group; the cross-sections are obtained thanks to a pre-homogenization step in a library processing code. Self-shielding calculation is necessary to correct cross-sections of resonant isotopes but is known to be a main source of error. Advanced self-shielding models as exposed in [1, 2] in conjunction with an optimization of the energy group mesh structure as proposed in [3] are incorporated in modern transport codes.

Another approach based on a Galerkin method is at the basis of the present work. Such a treatment of the energy had been first proposed in [4] with polynomial-based finite elements; however, the use of polynomial basis is not adapted to resonance singularities. We have proposed to handle this point by using wavelet basis. These function basis are obtained through a thresholding procedure applied to the Discrete Wavelet Transform (DWT) of a sampled cross-section or approximate flux in each group. The theoretical and implementation details of such a method can be found in [5]. This first study has revealed the interest of such an approach but also some questions. Although the number of coefficients to be kept, i.e. the size of the wavelet support considered, is relatively small, error on the final flux is not controlled and the extension of this method to heterogeneous cases is not straightforward. We propose a way to improve these two issues thanks to adaptive algorithms. Such procedures are embedded in within-group scattering iterations.

In Section 2, we first recall the framework of this first study and then describe the broad lines of the adaptive method. Results are presented in Section 3. Finally, Section 4 discusses properties a mesh should exhibit to improve the performances of such a method.

2. FRAMEWORK

A first series of tests are carried out on the fine structure equation which is a simplified form of the transport equation in an infinite, homogeneous medium under the Livolant-Jeanpierre hypotheses. The equation, where only the energy variable (or equivalently the lethargy u) remains, is written:

$$\left(\sigma_t^*(u) + \sigma_d\right)\varphi(u) = \sigma_d + r^*(\varphi(u)) \tag{1}$$

where r^* is the resonant collision operator defined as:

$$r^*(\varphi(u)) = \frac{1}{1-\alpha}\int_{u-\epsilon}^{u} du' e^{u'-u}\sigma_s^*(u')\varphi(u') \tag{2}$$

We have denoted respectively σ_s^* and σ_t^* the scattering and total microscopic cross-sections of the resonant isotope read in pointwise format (PENDF). σ_d is the dilution cross-section defined as $\sigma_d = \frac{\Sigma_t^+}{N^*}$, ratio of the macroscopic total non-resonant cross-section and the concentration of the resonant isotope.

Eq. 1 can be discretized in each lethargy group I_g (172-group XMAS mesh is used) thanks to a discontinuous finite element method using a wavelet basis $\left(g_m^g\right)_{m\in[1,N_g]}$ of $\left(L^2(I_g)\right)^{N_g}$. The weak formulation on a lethargy interval I_g is written in a matrix form:

$$H^g\Phi^g = \sum_{g'} S^{(g\leftarrow g')}\Phi^{g'} + F^g \tag{3}$$

with:

- Φ^g, vector containing the components of Φ in the wavelet basis
- H^g corresponding to the total interaction rate density:

$$H_{m,n}^g = \int_{I_g} du\sigma_t^{g*}(u)g_m^g(u)g_n^g(u) + \delta_{m,n}\sigma_d$$

- F^g representing a fixed source term:

$$F_m^g = \sigma_d\int_{I_g} du g_m^g(u)$$

- $S^{(g\leftarrow g')}$, the scattering source term, defined by:

$$S_{m,n}^{(g\leftarrow g')} = \frac{1}{1-\alpha}\int_{I_g} du g_m^g(u)\int_{I_{g'}\cap]u-\epsilon,u[} du' e^{u'-u}\sigma_s^*(u')g_n^{g'}(u')$$

Eq. 3 is solved using a Richardson iterative scheme as done for source iterations in the method of characteristics or discrete ordinate method:

$$H\Phi^{n+1} = S\Phi^n + F \tag{4}$$

In the spatially-dependent case, H is a block diagonal matrix originating from the spatial and angular integration of the transport equation in each group and S is assembled from the different $S^{(g \leftarrow g')}$ to consider scattering between groups.

In the remainder, we suppose that operators H and S have been calculated for a nearly full wavelet basis $(\phi_i)_{i\in\mathbb{N}}$.

3. ADAPTIVENESS

The aim of adaptiveness is double:

- improve the operators discretization at each iteration by selecting dynamically the basis functions and consequently, optimize the computational cost;
- guarantee an error bound for the final flux solution.

Matrices H_j (resp. S_j) used at iteration j are "extracted" from operator H (resp. S) with a support Λ_j^H (resp Λ_j^S) to be determined. Λ_j^H is the set of subscripts s.t. H_j is expressed on the wavelet basis $(\phi_i)_{i\in\Lambda_j^H}$. The main idea in the remainder is to choose this support in order to control the convergence.

3.1. Two-loop algorithm

A first algorithm with two iterative loops as given in [6] was implemented. The system solved at each iteration is written as

$$\Phi_{j+1}^{n+1} = A_{j+1}\left(S_{j+1}\Phi_{j+1}^n + F\right) \tag{5}$$

where $A = H^{-1}$. Iterations on j modify dynamically the support of the system solved whereas those on n are done with a quasi-constant support in order to make the Richardson iterative scheme converge to a given accuracy. The error can be expressed as:

$$\begin{aligned}\Phi_{j+1}^{n+1} - \Phi &= A_{j+1}\left(S_{j+1}\Phi_{j+1}^n + F\right) - A(S\Phi + F)\\ &= \left(A_{j+1} - A\right)\left(S_{j+1}\Phi_{j+1}^n + F\right) + A\left(S_{j+1} - S\right)\Phi_{j+1}^n + AS\left(\Phi_{j+1}^n - \Phi\right)\end{aligned}$$

which leads to a bound for the relative error:

$$\begin{aligned}\frac{\left\|\Phi_{j+1}^{n+1} - \Phi\right\|}{\left\|\Phi_{j+1}^{n+1}\right\|} \leq \frac{1}{1-\|AS\|}\Bigg(&\frac{\left\|\left(A_{j+1} - A\right)\left(S_{j+1}\Phi_{j+1}^n + F\right)\right\|}{\left\|\Phi_{j+1}^{n+1}\right\|} + \|A\|\frac{\left\|\left(S_{j+1} - S\right)\Phi_{j+1}^n\right\|}{\left\|\Phi_{j+1}^{n+1}\right\|} +\\ &\|AS\|\frac{\left\|\Phi_{j+1}^{n+1} - \Phi_{j+1}^n\right\|}{\left\|\Phi_{j+1}^{n+1}\right\|}\Bigg)\end{aligned} \tag{6}$$

A main issue is how to choose matrix S_{j+1} and A_{j+1} or, in other words, how to select the wavelet support. We clearly see that the error is monitored by two terms related to the number of coefficients kept for representing A and S operators and a third term involving the residual of the iteration. They are denoted respectively $\delta\epsilon^A$, $\delta\epsilon^S$ and $\delta\epsilon^{res}$. The main idea in the remainder is to monitor the errors related to the operator discretization using the numerical residual term in order to obtain a relation of the type:

$$\frac{\left\|\Phi_{j+1}^{n+1}-\Phi\right\|}{\left\|\Phi_{j+1}^{n+1}\right\|} \leq K \frac{\left\|\Phi_{j+1}^{n+1}-\Phi_{j+1}^{n}\right\|}{\left\|\Phi_{j+1}^{n+1}\right\|} \tag{7}$$

where K is a given constant. Error on the flux is thus controlled thanks to the numerical residual at each iteration.

$\delta\epsilon^S$ can be practically controlled by a thresholding on the product $S\Phi^n$ ensuring:

$$\left\|S_{j+1}\Phi_{j+1}^{n}-S\Phi_{j+1}^{n}\right\| \leq \epsilon_{j+1}\left\|\Phi_{j+1}^{n}\right\| \tag{8}$$

Coefficients kept give us the new support Λ_{j+1}^S growing slowly when decreasing ϵ_{j+1} thanks to wavelet properties. A similar procedure can be used for $\delta\epsilon^A$ ensuring:

$$\left\|(A_{j+1}-A)\left(S_{j+1}\Phi_{j+1}^{n}+F\right)\right\| \leq \epsilon'_{j+1}\left\|\Phi_{j+1}^{n}\right\| \tag{9}$$

Eq. 6 then becomes:

$$\frac{\left\|\Phi_{j+1}^{n+1}-\Phi\right\|}{\left\|\Phi_{j+1}^{n+1}\right\|} \leq \frac{1}{1-\|AS\|}\left(\epsilon'_{j+1}\frac{\left\|\Phi_{j+1}^{n}\right\|}{\left\|\Phi_{j+1}^{n+1}\right\|}+\epsilon_{j+1}\|A\|\frac{\left\|\Phi_{j+1}^{n}\right\|}{\left\|\Phi_{j+1}^{n+1}\right\|}+\|AS\|\frac{\left\|\Phi_{j+1}^{n+1}-\Phi_{j+1}^{n}\right\|}{\left\|\Phi_{j+1}^{n+1}\right\|}\right) \tag{10}$$

As proposed in [6], a geometrical decreasing sequence of (ϵ_j) is fixed and iterations on n are performed until the residual term becomes inferior to the value imposed by this sequence. ϵ_j and ϵ'_j are set in order to ensure that the first two terms defined in Eq. 6 decays at the same rate i.e.

$$\epsilon'_{j+1}=\frac{\epsilon_{j+1}}{\|A\|} \tag{11}$$

At a given j, Richardson iterations are carried out until

$$\frac{\left\|\Phi_{j+1}^{n+1}-\Phi_{j+1}^{n}\right\|}{\left\|\Phi_{j+1}^{n+1}\right\|} \leq \frac{\epsilon_{j+1}}{\|AS\|} \tag{12}$$

Thus, the relative error on the flux is bounded by the sequence $(NB)_j$ directly linked to the decreasing sequence of $(\epsilon)_j$:

$$\frac{\left\|\Phi_{j+1}^{n+1}-\Phi\right\|}{\left\|\Phi_{j+1}^{n+1}\right\|} \lesssim \frac{3}{1-\|AS\|}\epsilon_{j+1}=NB_{j+1} \tag{13}$$

considering

$$\left\|\Phi_{j+1}^{n+1}\right\| \approx \left\|\Phi_{j+1}^{n}\right\| \tag{14}$$

The choice of (ϵ_j) is arbitrary and some numerical tests are performed with different sequences. A possibility is to choose

$$\epsilon=\frac{\epsilon_{j+1}}{\epsilon_j}=\|A_jS_j\|=\rho_j$$

the rate of convergence of Richardson method.

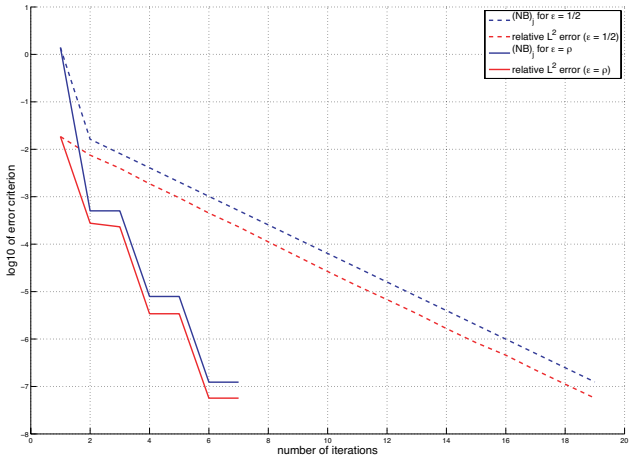

Figure 1. Error behaviour for different ϵ values on groups 26 to 29 of ^{16}O

Two different phenomena can occur depending on the ϵ value compared to $\|AS\|$ as presented in Fig. 1 for ^{16}O where $\|AS\| = 0.01$:

- $\epsilon >> \|AS\|$ (case $\epsilon = 1/2$ in Fig. 1): Richardson iterative scheme converges rapidly (in one iteration in the case presented) and the error decreases linearly at the same rate than the sequence $(\epsilon)_j$ but it needs many outer iterations. In our example, the slope of the straight line is equal to $-0.3 = log_{10}(1/2)$.
- $\epsilon << \|AS\|$: The number of coefficients kept increases rapidly and several Richardson iterations are necessary to converge at a given support.

The case $\epsilon = \rho$ in Fig. 1 is an intermediate choice. A compromise has to be found between increasing too slowly the support causing useless outer iterations and keeping too many coefficients which leads to the resolution of a uselessly large linear system. This choice is discussed in Subsection 3.3.

3.2. One-loop algorithm

A second algorithm is proposed as a simplification of the previous one with only one level of iterations to be closer of what is classically done for source iterations. It implies to control at the same time the evolution of the supports and the residual. Eq. 3 is written as:

$$\Phi^{n+1} = A^{n+1}\left(S^{n+1}\Phi^n + F\right) \tag{15}$$

Eqs. 3 and 15 imply the following relationships:

$$\begin{cases} (I - AS)\left(\Phi^{n+1} - \Phi\right) = \left(A^{n+1} - A\right)\left(S^{n+1}\Phi^n + F\right) + A\left(S^{n+1} - S\right)\Phi^n - AS\left(\Phi^{n+1} - \Phi^n\right) \\ \Phi^{n+1} - \Phi^n = \left(A^{n+1} - A^n\right)\left(S^{n+1}\Phi^n + F\right) + A^n\left(S^{n+1} - S^n\right)\Phi^n + A^nS^n\left(\Phi^n - \Phi^{n-1}\right) \end{cases}$$

And thus, the error is controlled thanks to an inequality similar to Eq. 6 for the two-loop algorithm:

$$\begin{aligned}\|I - AS\| \left\|\Phi^{n+1} - \Phi\right\| &\leq \left\|\left(A^{n+1} - A - AS\left(A^{n+1} - A^n\right)\right)\left(S^{n+1}\Phi^n + F\right)\right\| \\ &\quad + \left\|A\left(\left(S^{n+1} - S\right) - SA^n\left(S^{n+1} - S^n\right)\right)\Phi^n\right\| \\ &\quad + \left\|ASA^nS^n\left(\Phi^n - \Phi^{n-1}\right)\right\| \\ &\leq \delta\epsilon^A + \delta\epsilon^S + \delta\epsilon^{res} \end{aligned} \tag{16}$$

Such a bound for the operator-related error $\delta\epsilon^S$ (resp. $\delta\epsilon^A$) is interesting because it takes into account both $\|S^{n+1} - S\|$ (resp. $\|A^{n+1} - A\|$), the distance between the current operator and the complete one and $\|S^{n+1} - S^n\|$ (resp. $\|A^{n+1} - A^n\|$), the distance between two successive operators. As the first term decreases with n until 0, the second one increases until $\|S - S^n\|$ (resp. $\|A - A^n\|$). So, we have, for example for $\delta\epsilon^S$:

$$\delta\epsilon^S_{(S^{n+1}=S^n)} = \delta\epsilon^S_{init} = \|A\left(S^n - S\right)\Phi^n\| \tag{17}$$

$$\delta\epsilon^S_{(S^{n+1}=S)} = \delta\epsilon^S_{last} = \|ASA^n\left(S - S^n\right)\Phi^n\| \tag{18}$$

As $\|AS\| < 1$ (ensuring the convergence of Richardson iterations), we guarantee:

$$\delta\epsilon^S_{last} < \delta\epsilon^S_{init} \tag{19}$$

The error bounds defined by Eq. 16, $\delta\epsilon^S_{init}$ and $\delta\epsilon^S_{last}$ are at the basis of our algorithm. Three different situations can occur between two iterations:

- $\delta\epsilon^{res} \in [\delta\epsilon^S_{last}, \delta\epsilon^S_{init}]$. It is possible to decrease the error due to operator S discretization to the numerical residual, so, we choose S^{n+1} to ensure $\delta\epsilon^S = \delta\epsilon^{res}$;
- $\delta\epsilon^{res} < \delta\epsilon^S_{last}$. Numerical residual is too small to be reached directly. Error on operator S is reduced to
$$\delta\epsilon^S = \alpha\delta\epsilon^S_{init} + (1 - \alpha)\delta\epsilon^S_{last} \tag{20}$$
with α fixed $\in]0, 1[$;
- $\delta\epsilon^{res} > \delta\epsilon^S_{init}$. The numerical residual is not yet enough converged, so, we do not modify the support of operator, $S^{n+1} = S^n$.

With such an approach, even if we do not know the behaviour of $\delta\epsilon^S_{(S^{n+1})}$ between $\delta\epsilon^S_{init}$ and $\delta\epsilon^S_{last}$ (strictly decreasing or having a minimum or a maximum), we ensure that the error monotonically decreases and so the convergence of the algorithm. In a first version of the algorithm, we apply to A the same procedure as detailed for S (by replacing $\delta\epsilon^S$ by $\delta\epsilon^A$ and $\delta\epsilon^{res}$ by $\delta\epsilon^S$).

The only remaining parameter is α. A numerical study is performed to give some tendencies for its selection.

3.3. Efficiency and extension to spatially-dependent configurations

One of the goal of adaptiveness referred to in the introduction is the improvement of the algorithm efficiency. In this context, a measure of the computational cost is defined by:

$$cost = \sum_j \sum_n \left(\Lambda^S_{j,n} + \Lambda^A_{j,n}\right) \tag{21}$$

where $\Lambda^S_{j,n}$ (resp. $\Lambda^A_{j,n}$) represents the support size of operator S^n_j (resp. A^n_j) at iteration j, n.

In the general case, the costful operation is the angular-spatial resolution, i.e. obtaining matrix H^{-1}. As soon as this matrix is known, the cost of source iterations is directly linked to the size of operators manipulated: $\Lambda^S_{j,n}$ construction of matrix S^n_j and $\Lambda^A_{j,n}$ the order of the system used for the flux calculation. It justifies the use of Eq. 21 as a measure of the cost of algorithms.

Minimizing the cost is the guideline to choose the remaining parameters, the decreasing sequence (ϵ_j) for the two-loop algorithm and the reduction rate α for the single-loop one.

The representation of the cost as a function of ϵ in Fig. 2 for the groups 26 to 29 of ^{16}O underlines the importance of judiciously selecting the rate of decay. The choice of $\epsilon_j = \|A_j S_j\|$ seems relevant for all cases studied as illustrated for ^{16}O in Fig. 2 where $\|AS\| = 0.01$. Note that $\|A_j S_j\|$ converges rapidly to $\|AS\|$.

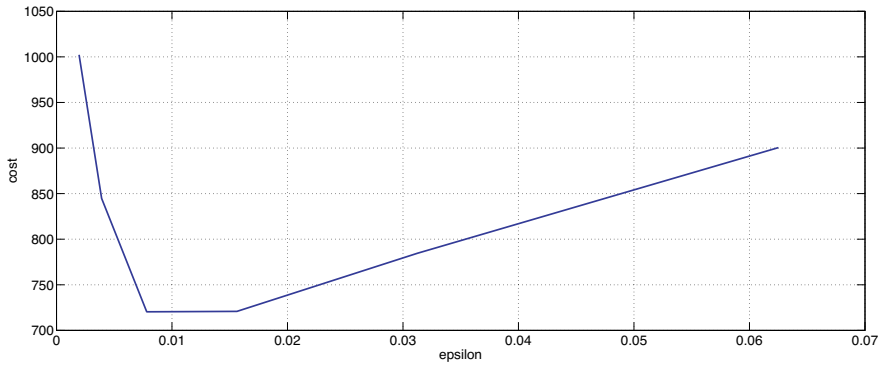

Figure 2. Cost for different ϵ values for a given accuracy of $\mathbf{10^{-6}}$ for groups 26 to 29 of ^{16}O

Remarks are similar for the choice of the parameter α in the single-loop algorithm as shown in Fig. 3 . If not enough coefficients are kept at each iteration, the error decreases slowly which causes an important cost. On the opposite, if an important number is kept, large systems have to be solved uselessly. An interesting compromise seems to keep coefficients in order to reduce the error by about half ($\alpha = 0.5$).

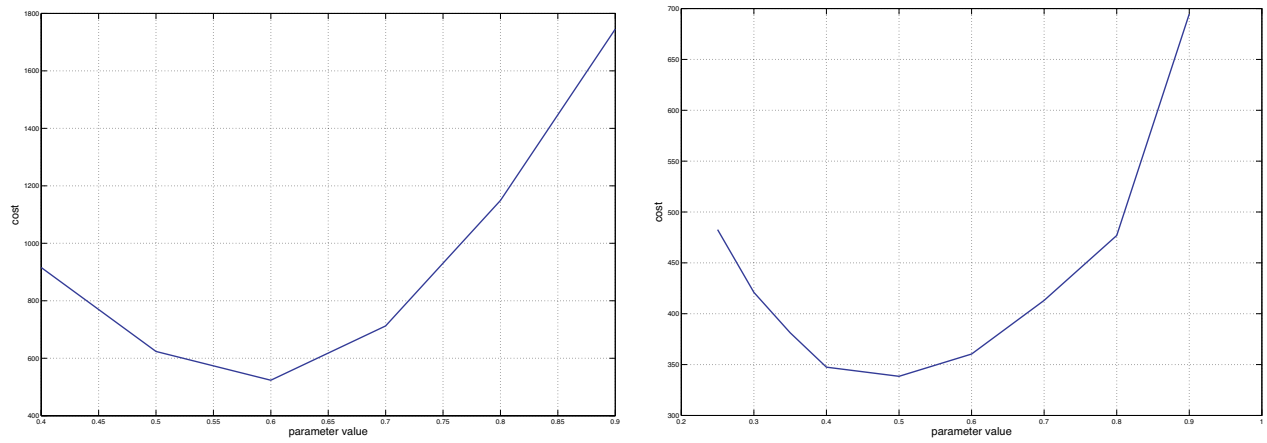

Figure 3. Cost of the algorithm depending on the parameter α value for a given accuracy $\epsilon = \mathbf{10^{-5}}$ on group 56 of ^{56}Fe (left) and $\epsilon = \mathbf{10^{-4}}$ on group 88 of ^{238}U (right)

When these parameters have been selected, the algorithms can be tested on the fine structure equation. However, the treatment of the error related to operator A is not extensible to spatially-dependent problems. A simple alternative consists in using for A the same support as the one obtained for S. Fig. 4 presents the number of coefficients kept for each operators on the previous algorithm and the accuracy obtained at each iteration. Let us note that, for a standard accuracy of 10^{-3}, the support of S is greater than the H one and consequently, using S support for A discretization should be a conservative choice. Obviously, because of this strategy some coefficients kept for operator S are not necessary because there is a ratio of $\|A\|$ between $\delta\epsilon^A$ and $\delta\epsilon^S$ (Eq. 10). The cost is increased but convergence is not disturbed for an accuracy of about 10^{-3}. This simple approach seems a good starting point to handle spatially-dependent cases.

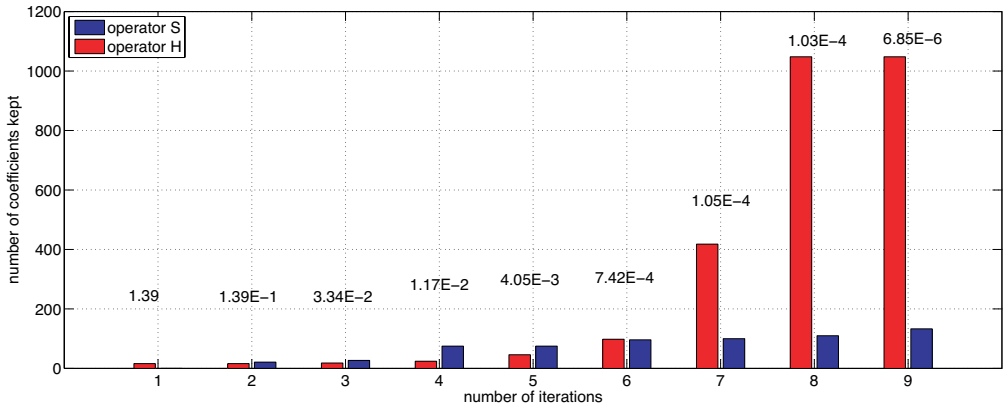

Figure 4. Comparison of the number of coefficients kept on operators **S** and **H** for group 88 of ^{238}U

Let us now compare the results obtained with the different algorithms. All these tests are performed with the optimal thresholding strategy proposed in [5] (use of Canuto's thresholding

on the Bondarenko flux with symmlets of 6^{th} order).

Table I summarizes the different strategies used in Figs. 5 and 6 on the group 88 of ^{238}U and 56 of ^{56}Fe in order to compare the algorithms.

Table I. Strategies used in Figs. 5 and 6 to compare the different algorithms

Adaptive Algorithms			Non Adaptive Algorithm $(\star)$
	2 thresholding procedures (on S and A operators)	1 thresolding procedure (S support used for A operator)	
2 levels of iterations (one for the support and one for Richardson)	solid blue line	solid red line	solid magenta line
1 level of iterations	dashed blue line	dashed red line	

$(\star)$ calculation is done in order to have an optimal cost by limiting the number of Richardson iterations such that $\delta\epsilon^{res}$ is of the same order as $\delta\epsilon^S + \delta\epsilon^A$

With these two cases, the influence of $\|AS\|$ on the convergence of the different algorithms can be studied. For ^{238}U case, $\|AS\| = 0.27$ whereas $\|AS\| = 0.08$ for ^{56}Fe case. In the two-loop algorithm (resp. one-loop algorithm), the convergence behaviour is relatively independant of $\|AS\|$ when using $\epsilon = \|AS\|$ (resp. Eq. 20) for controlling $\delta\epsilon^S$ and $\delta\epsilon^A$. It explains similarities between Fig. 5 and Fig. 6. Our algorithms seem to be of a general interest whatever the isotope and energy range are.

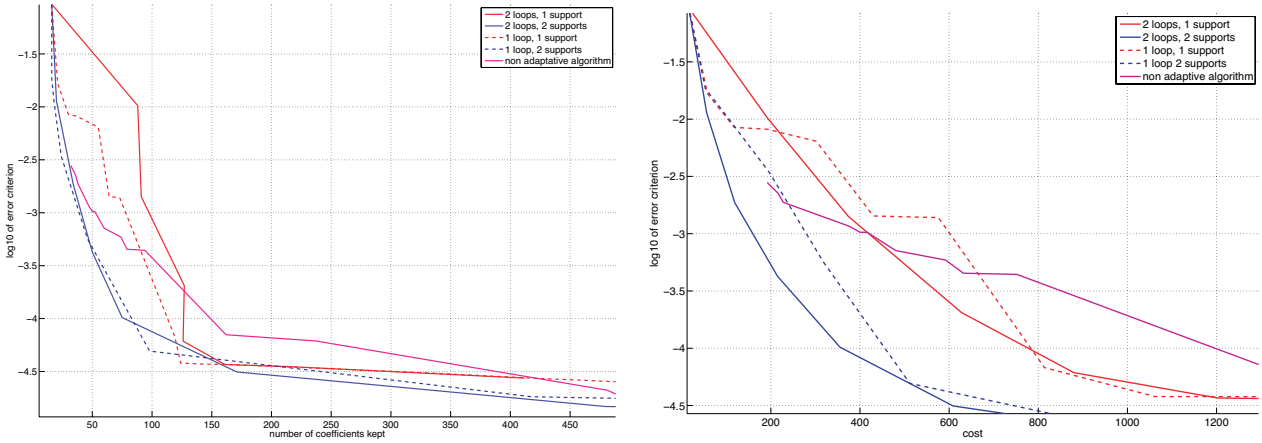

Figure 5. Comparison of algorithms in terms of convergence (left) and cost (right) for group 88 of ^{238}U with $\sigma_{\mathbf{d}} = \mathbf{100}$ barn - Relative $\mathbf{L^2}$-norm error used

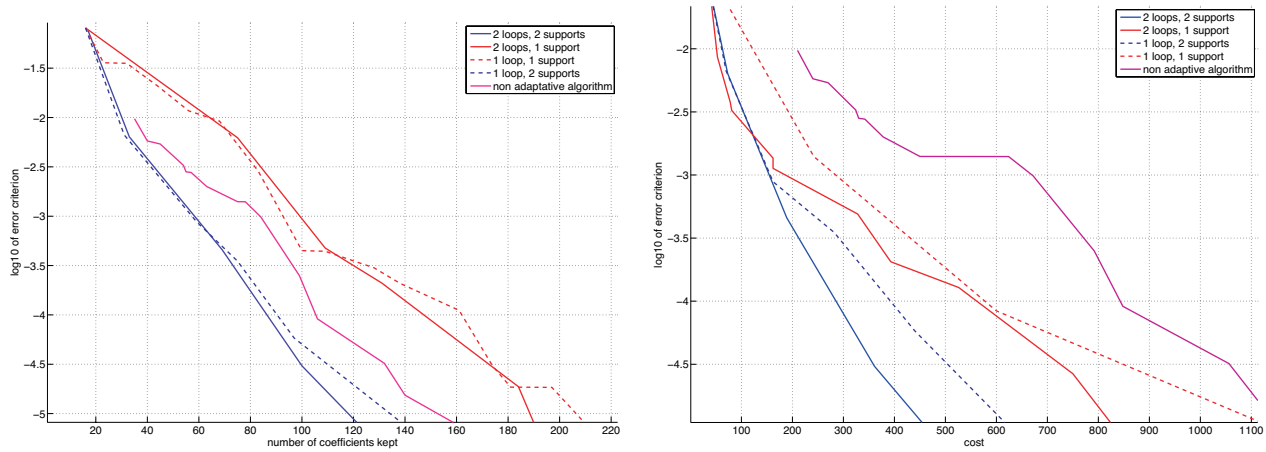

Figure 6. Comparison of algorithms in terms of convergence (left) and cost (right) for group 56 of ^{56}Fe with $\sigma_{\mathbf{d}} = \mathbf{100}$ barn - Relative $\mathbf{L^2}$-norm error used

These Figures also underline that the algorithms with one or two loops give similar performances. The simplified algorithm only slightly deteriorate the convergence and the cost. However, when using a unique support for A and S, the convergence can be significantly deteriorated. As expected, the cost is increased by this simplification. The difference between adaptive and non adaptive algorithms is more important for ^{56}Fe due to one additional iteration. Improvements relatively to the cost are significant because the cost presented in Figs. 5 and 6 for the non adpative algorithm is a nearly optimal one and requires a control of the different error terms ($\delta\epsilon^{res}$, $\delta\epsilon^{A}$ and $\delta\epsilon^{S}$).

Furthermore, adaptive schemes present other advantages. In the perspective of spatially-dependent cases, it allows to consider a different support in each region and thus to keep only a low number of coefficients in parts without resonances. Moreover, the error is monitored on the final flux thanks to an a priori estimator contrarily to the non-adaptive algorithm.

4. ENERGY MESH

The previous study was done using the XMAS mesh which had not been devised for a wavelet-based method and has to be questioned. In this section, we give properties a mesh should exhibit in order to decrease the number of coefficients used for a given accuracy. Fig. 7 represents, on the left, the cross-section as a function of lethargy and the group limits in the XMAS mesh for groups 86 to 88 of ^{238}U and 81 to 83 of ^{239}Pu. We compare the convergence of the relative error $\epsilon = r/\left\|\Phi_{ref}\right\|_{L^2(I_{\tilde{g}})}$ with respect to the number N of coefficients kept by considering the XMAS mesh and a mesh where the XMAS groups (e.g. 86 to 88 for ^{238}U) have been collapsed into a single one ($\tilde{g} = \bigcup_g g$). r and N are given in Table II for each mesh to ensure a proper comparison.

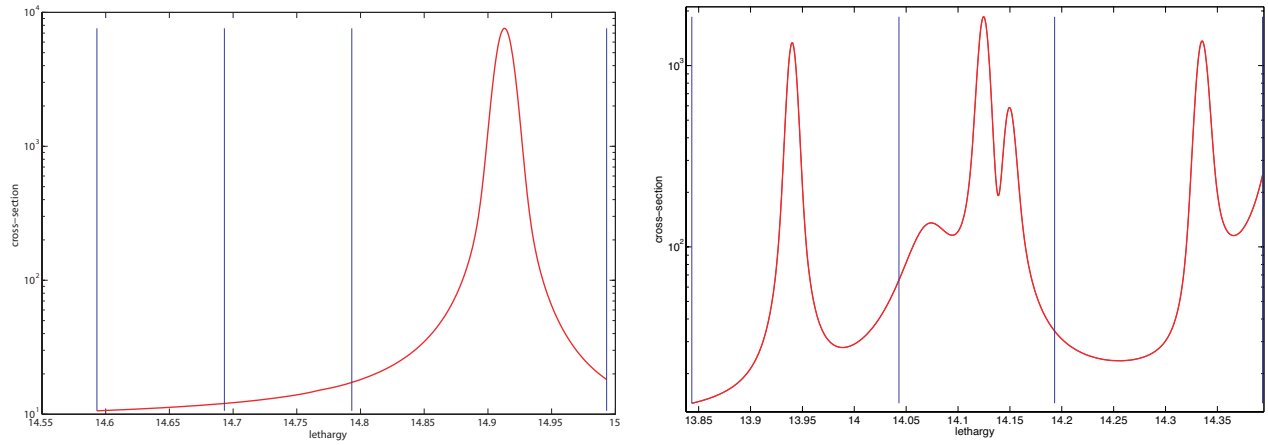

Figure 7. Representation of groups 86 to 88 of ^{238}U (left) and 81 to 83 of ^{239}Pu (right)

Table II. Definition of the number of coefficients N and error r used in the comparison of the XMAS and collapsed meshes

mesh	N	r
XMAS	$\sum_{g\in\tilde{g}} N_g$	$\sqrt{\sum_{g\in\tilde{g}} \left\|\Phi^g - \Phi^g_{ref}\right\|^2_{L^2(I_g)}}$
collapsed	$N_{\tilde{g}}$	$\left\|\Phi^{\tilde{g}} - \Phi^{\tilde{g}}_{ref}\right\|_{L^2(I_{\tilde{g}})}$

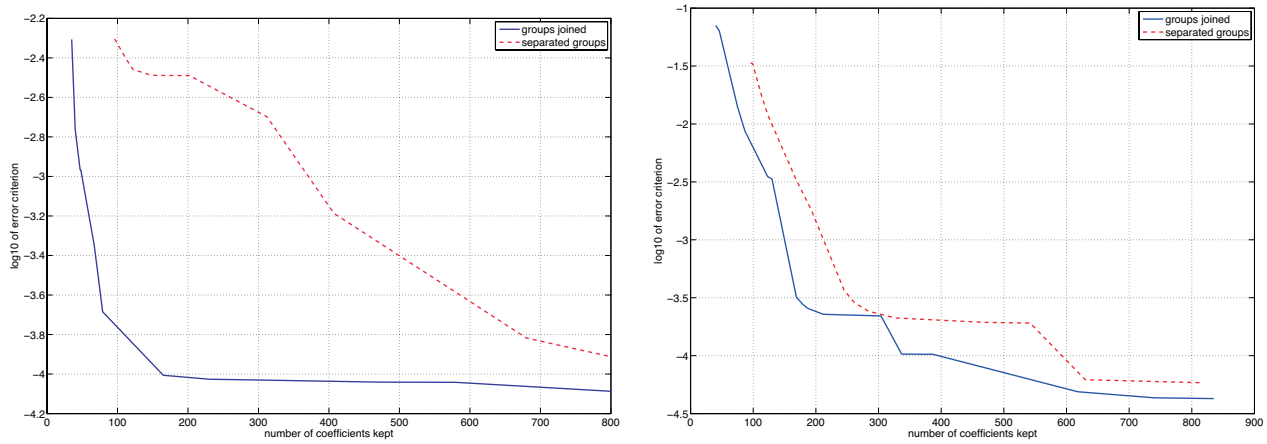

Figure 8. Comparison of the convergence on relative $\mathbf{L^2}$-norm error by considering three distincts groups or only one group for groups 86 to 88 of ^{238}U (left) and groups 81 to 83 of $^{\mathbf{239}}\mathbf{Pu}$ (right)

If wavelets are well adapted to represent resonances, it is clear that they are not optimal for groups with small variations. It explains why the convergence rate is higher with only one group instead of using the three groups of the XMAS mesh. If groups are more perturbated as it is the case for groups 81 to 83 of ^{239}Pu, the difference is less pronounced.

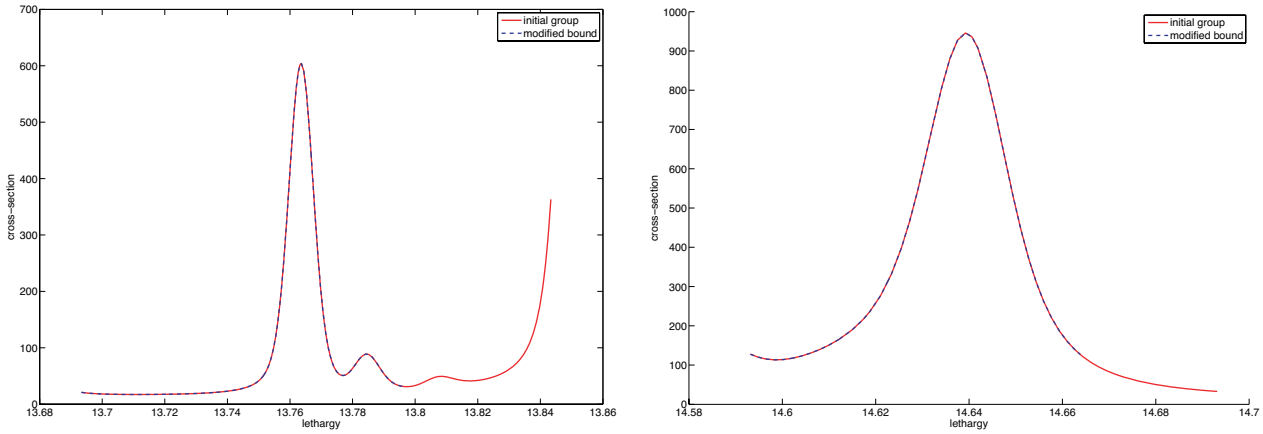

Figure 9. Group 80 (left) and 86 (right) of ^{235}U and modified bound

Another aspect that seems interesting to discuss is group boundaries. Actually, the use of a periodic cascade algorithm for the DWT can create parasite oscillations at the boundaries and let us think that the nearest the two boundary values, the better the convergence. We take as example group 80 of ^{235}U which contains a part of the resonance of the following group on its right boundary and group 86 where the two bounds are slightly different. Fig. 9 presents these groups and the modified ones we consider to study impact of boundaries. Fig. 10 presents the rate of decay for these two examples. Having the left and right bound equivalent does not seem as important as the group size. Results are close with the initial bound or the modified one.

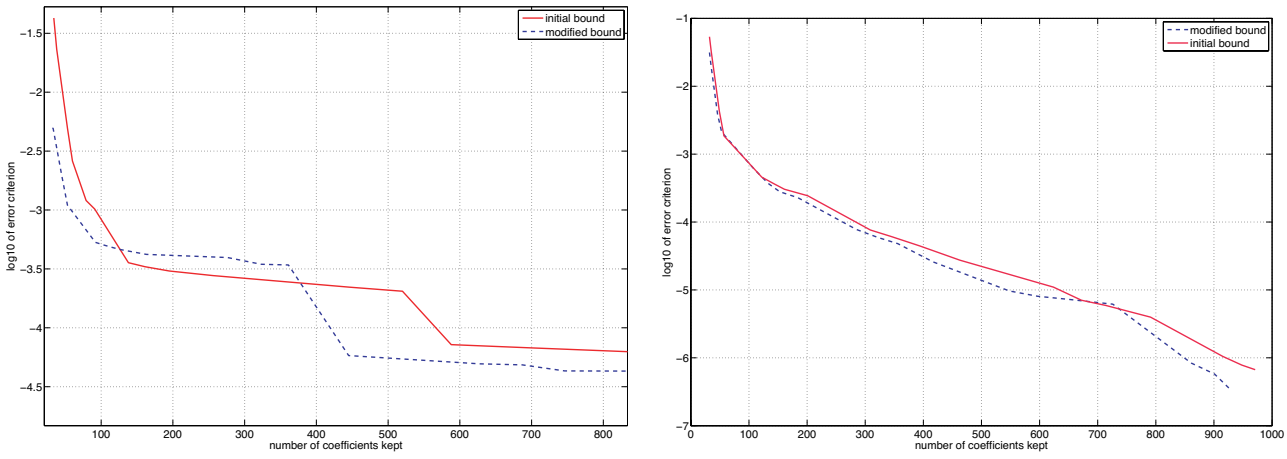

Figure 10. Comparison of the convergence for group 80 (left) and 86 (right) of ^{235}U by considering the whole group and a group with a modified bound

The most significant aspect concerning the energy mesh seems to be the length of groups. Groups where the cross-sections exhibit low variations or without any resonance are not adapted to a wavelet method and have to be merged with their neighbours for the sake of effectiveness.

5. CONCLUSIONS

Adaptive algorithms were proposed for a wavelet-based self-shielding method thanks to a priori error estimates. Tests were performed in the case of the fine structure equation and modifications necessary for spatially-dependent test-cases have been discussed. The method we proposed presents three main advantages: the control, at least partial, of the error on the flux solution, the capability to treat heterogeneous configurations and the optimization of the computational cost. In addition, properties a mesh should exhibit to improve convergence were discussed and it has been shown that the group size is a predominant parameter.

Implementing the algorithm in the spatially-dependent case is now necessary to assess its actual capability and for further comparisons. Additional developments on meshing could also be interesting to devise an optimized mesh.

REFERENCES

[1] A. Hébert, "A review of legacy and advanced self-shielding models for lattice calculation", *Nuclear Science and Engineering*, **155**, no. 2, pp. 310-320 (2007).

[2] P. Reuss and M. Coste-Delclaux, "Development of computational models used in France for neutron resonance absorption in light water lattices", *Progress in Nuclear Energy*, **42**, no. 3, pp. 237-282 (2003).

[3] N. Hfaiedh, *Nouvelle Méthodologie de Calcul de l'Absorption Résonnante*, Ph.D. thesis, Université Louis Pasteur Strasbourg, France (September 21, 2006).

[4] E.J. Allen, "A Finite Element Approch for Treating the Energy Variable in the Numerical Solution of the Neutron Transport Equation", *Transport Theory Stat. Phys.*, **15**, pp. 449-478 (1986).

[5] R. Le Tellier, D. Fournier and J.M. Ruggieri "A Wavelet-Based Finite Element Method for the Self-Shielding Issue in Neutron Transport", *Nuclear Science and Engineering* (accepted)

[6] A. Cohen, *Numerical Analysis of Wavelet Methods*, Studies in Mathematics and its Application, D.N. Arnold, P.G. Ciarlet, P.L. Lions, H.A Van Der Vorst Editors (2003).